10. Kassis AI. Toxicity and therapeutic effects of low-energy electrons. *Nucl Instrum Meth Phys Res [B]* 1994;87:279–284.
11. Kassis AI, Adelstein SJ. Preclinical animal studies with radiolabeled IUdR. *J Nucl Med* 1996;37:343–352.
12. Kassis AI, Van den Abbeele AD, Wen PYC, et al. Specific uptake of the Auger electron-emitting thymidine analogue 5-[^{123}I/^{125}I]iodo-2′-deoxyuridine in rat brain tumors: diagnostic and therapeutic implications in humans. *Cancer Res* 1990;50:5199–5203.
13. Sufrin G, Meyer JS, Martin SA, Schechtman K. Proliferative activity of urothelium and tumors of renal pelvis, ureter, and urinary bladder evaluated by thymidine labeling. *Urology* 1984;23(suppl):15–22.
14. Hicks RM, Wakefield JSJ. Rapid induction of bladder cancer in rats with N-methyl-N-nitrosourea. I. Histology. *Chem Biol Interact* 1972;5:139–152.
15. Baranowska-Kortylewicz J, Kinsey BM, Layne WW, Kassis AI. Radioiodo-demercuration: a simple synthesis of 5-[$^{123/125/127}$I]iodo-2′-deoxyuridine. *Appl Radiat Isot* 1988;39:335–341.
16. Eidinoff ML, Cheong L, Rich MA. Incorporation of unnatural pyrimidine bases into deoxyribonucleic acid of mammalian cells. *Science* 1959;129:1550–1551.
17. Morris NR, Cramer JW. DNA synthesis by mammalian cells inhibited in culture by 5-iodo-2′-deoxyuridine. *Mol Pharmacol* 1966;2:1–9.
18. Calabresi P, Cardoso SS, Finch SC, et al. Initial clinical studies with 5-iodo-2′-deoxyuridine. *Cancer Res* 1961;21:550–559.
19. Hughes WL, Commerford SL, Gitlin D, et al. Deoxyribonucleic acid metabolism in vivo. I. Cell proliferation and death as measured by incorporation and elimination of iododeoxyuridine. *Fed Proc* 1964;23:640–648.
20. Commerford SL. Biological stability of IUdR labeled with ^{125}I after incorporation into the DNA of the mouse. *Nature (London)* 1965;206:949–950.
21. Kassis AI, Sastry KSR, Adelstein SJ. Kinetics of uptake, retention and radiotoxicity of ^{125}IUdR in mammalian cells: implications of localized energy deposition by Auger processes. *Radiat Res* 1987;109:78–89.
22. Prusoff WH. A review of some aspects of 5-^{125}I-iododeoxyuridine and azauridine. *Cancer Res* 1963;23:1246–1259.
23. Klecher RW Jr, Jenkins JF, Kinsella TJ, Fine RL, Strong JM, Collins JM. Clinical pharmacology of 5-iodo-2′-deoxyuridine and 5-iodouracil and endogenous pyrimidine modulation. *Clin Pharmacol Ther* 1985;38:45–51.
24. Hofer KG, Harris CR, Smith JM. Radiotoxicity of intracellular ^{67}Ga, ^{125}I and ^{3}H: nuclear versus cytoplasmic radiation effects in murine L1210 leukaemia. *Int J Radiat Biol* 1975;28:225–241.
25. Kassis AI, Fayad F, Kinsey BM, Sastry KSR, Taube RA, Adelstein SJ. Radiotoxicity of ^{125}I in mammalian cells. *Radiat Res* 1987;111:305–318.
26. Makrigiorgos GM, Kassis AI, Baranowska-Kortylewicz J, et al. Radiotoxicity of 5-[^{123}I]iodo-2′-deoxyuridine in V79 cells: a comparison with 5-[^{125}I]iodo-2′-deoxyuridine. *Radiat Res* 1989;118:532–544.
27. Warters RL, Hofer KG, Harris CR, Smith JM. Radionuclide toxicity in cultured mammalian cells: elucidation of the primary site of radiation damage. *Curr Top Radiat Res Q* 1977;12:389–407.
28. Hofer KG, Hughes WL. Radiotoxicity of intranuclear tritium, ^{125}iodine and ^{131}iodine. *Radiat Res* 1971;47:94–109.
29. Bradley EW, Chan PC, Adelstein SJ. The radiotoxicity of iodine-125 in mammalian cells I. Effects on the survival curve of radioiodine incorporated into DNA. *Radiat Res* 1975;64:555–563.
30. Chan PC, Lisco E, Lisco H, Adelstein SJ. The radiotoxicity of iodine-125 in mammalian cells II. A comparative study on cell survival and cytogenetic responses to ^{125}IUdR, ^{131}IUdR and ^{3}HTdR. *Radiat Res* 1976;67:332–343.
31. Sundell-Bergman S, Johanson KJ. Repairable and unrepairable DNA strand breaks induced by decay of ^{3}H and ^{125}I incorporated into DNA of mammalian cells. *Radiat Environ Biophys* 1980;18:239–248.
32. Kassis AI, Adelstein SJ, Haydock C, Sastry KSR. Radiotoxicity of ^{75}Se and ^{35}S: theory and application to a cellular model. *Radiat Res* 1980;84:407–425.
33. Kassis AI, Adelstein SJ, Haydock C, Sastry KSR, McElvany KD, Welch MJ. Lethality of Auger electrons from the decay of bromine-77 in the DNA of mammalian cells. *Radiat Res* 1982;90:362–373.
34. Kassis AI, Adelstein SJ, Haydock C, Sastry KSR. Thallium-201: an experimental and a theoretical radiobiological approach to dosimetry. *J Nucl Med* 1983;24:1164–1175.
35. Kassis AI, Sastry KSR, Adelstein SJ. Intracellular distribution and radiotoxicity of chromium-51 in mammalian cells: Auger-electron dosimetry. *J Nucl Med* 1985;26:59–67.
36. Kassis AI, Howell RW, Sastry KSR, Adelstein SJ. Positional effects of Auger decays in mammalian cells in culture. In: Baverstock KF, Charlton DE, eds. *DNA damage by Auger emitters*. London: Taylor & Francis, Ltd.; 1988:1–13.
37. Mariani G, Di Sacco S, Volterrani D, et al. Intra-arterial infusion of 5-[^{123}I]iodo-2′-deoxyuridine in patients with inoperable liver metastases from colorectal cancer. In: *Program and Abstracts of the Forty-second Annual Meeting of the Radiation Research Society*, Nashville, TN; April 29–May 4, 1994:208.
38. Harrison K, Dalrymple GV, Baranowska-Kortylewicz J. Bladder cancer-[123I]IUdR imaging in preparation for [125I]IUdR therapy [Abstract]. *J Nucl Med* 1994;35:144P.
39. Herr HW, Laudone VP, Whitmore WF, Jr. An overview of intravesical therapy for superficial bladder tumors. *J Urol* 1987;138:1363–1368.
40. Catalona WJ, Hudson MA, Gillen DP, Andriole GL, Ratliff TL. Risks and benefits of repeated courses of intravesical bacillus Calmette-Guerin therapy for superficial bladder cancer. *J Urol* 1987;137:220–224.
41. Shaw GL, Mulshine JL. Biomarkers in early detection of lung cancer. *Contemp Oncol* July/August 1991;43–51.

Feasibility of Fluorine-18-Fluorophenylalanine for Tumor Imaging Compared with Carbon-11-L-Methionine

Kazuo Kubota, Kiichi Ishiwata, Roko Kubota, Susumu Yamada, Jutaro Takahashi, Yoshinao Abe, Hiroshi Fukuda and Tatsuo Ido

Department of Nuclear Medicine and Radiology, Institute of Development, Aging and Cancer and Cyclotron and Radioisotope Center, Tohoku University, Sendai, Japan; and Tokyo Metropolitan Institute for Gerontology, Tokyo, Japan

L-[methyl-^{11}C]methionine (^{11}C-Met) is a useful tracer for tumor imaging with PET. The drawbacks include a short half-life and high physiological accumulation in abdominal organs. To overcome these shortfalls, the feasible use of [^{18}F]fluorophenylalanine (^{18}F-Phe), which shares the same amino acid transport system with Met, for tumor imaging was examined. **Methods:** The time course of tissue distribution of ^{18}F-Phe and the tumor uptake response to radiotherapy were compared with ^{14}C-Met and [^{3}H] thymidine (^{3}H-Thd) in the rat AH109A tumor model. Intratumoral distribution of ^{18}F-Phe was compared with ^{14}C-Met and ^{14}C-Thd using double-tracer macroautoradiography (ARG). We also evaluated whole-body ARG. **Results:** Tumor uptake of ^{18}F-Phe peaked at 60 min postinjection and was higher than that of the liver, intestine and kidney but lower than the pancreas. Tumor uptake of ^{18}F-Phe was similar to that of ^{14}C-Met. Tumor-to-blood and tumor-to-muscle ratios were higher in ^{14}C-Met compared with that of ^{18}F-Phe because of the rapid blood clearance of ^{14}C-Met. With whole-body ARG, the tumor was clearly visualized with high contrast. Radiotherapeutic response of tumor uptake of ^{18}F-Phe was as rapid as that with ^{14}C-Met and with ^{3}H-Thd. Intratumoral distribution of ^{18}F-Phe and ^{14}C-Met were identical, and ^{18}F-Phe and ^{14}C-Thd were similar. **Conclusion:** Fluorine-18-Phe seems to be a potentially useful amino acid tracer for tumor imaging with a longer half-life than ^{11}C, with higher tumor contrast in the abdomen than Met and a similar sensitive response to radiotherapy.

Key Words: fluorine-18-fluorophenylalanine; autoradiography; carbon-11-methionine; PET; fluorine-18-FDG

J Nucl Med 1996; 37:320–325

A glucose analog, ^{18}F-2-fluoro-2-deoxy-D-glucose (FDG), and an essential amino acid tracer, L-[methyl-^{11}C]methionine (^{11}C-Met), have been used for tumor imaging with PET. Carbon-11-Met is useful for the diagnosis of the brain (*1*), head

Received Dec. 27, 1994; revision accepted Jun. 7, 1995.

For correspondence or reprints contact: Kazuo Kubota, MD, Department of Nuclear Medicine and Radiology, Institute of Development, Aging and Cancer, Tohoku University, 4-1 Seiryomachi, Aoba-ku, Sendai 980-77, Japan.

and neck (*2*), lung (*3*) and breast tumors (*4*), as well as lymphomas (*5*). Since physiological accumulation of ^{11}C-Met in normal brain tissue is minimal, resulting in high-contrast delineation of brain tumors, assessing the extent of glioma is possible (*6*). Whereas, FDG-PET is also useful for grading brain malignancies (*7*) and diagnosing abdominal tumors (*8,9*). The use of ^{11}C-Met to image abdominal tumors, however, is hampered by its high accumulation in the liver, pancreas and intestine, thus reducing the contrast of tumor to the background (*10,11*).

In pituitary adenomas, rapid response of ^{11}C-Met uptake following hormonal therapy has been reported (*12*). Rapid and sensitive responses of tumor uptake of ^{11}C-Met to radiochemotherapy have also been reported in glioma (*13*), lung (*14*) and breast cancers (*15*). Experimental studies have demonstrated that tumor uptake of ^{11}C-Met is more sensitive to radiotherapy compared to FDG (*16*). Within the tumor, accumulation of ^{14}C-Met is highly cancer-cell-specific, while accumulation of FDG is high in macrophages and granulation tissue as well as cancer cells (*17*). These studies point to the usefulness of ^{11}C-Met-PET for monitoring treatment of cancer. The short half-life of ^{11}C-Met (20 min), however, necessitates in-house synthesis and/or rapid delivery, in addition to its unsuitability for treatment evaluation of abdominal tumors.

L-[2-^{18}F]fluorotyrosine (^{18}F-Tyr) is an amino acid tracer with a long half-life, suitable for measuring the rate of protein synthesis (*18*). Weinhard et al. (*19*) demonstrated that the use of ^{18}F-Tyr with PET caused a high accumulation of ^{18}F-Tyr in brain tumors mediated by increased transport rate rather than by protein synthesis rate (*19*). We have previously demonstrated that the accumulation of 3,4-dihydroxy-2-[^{18}F]fluoro-L-phenylalanine (*20*) or 4-borono-2-[^{18}F]fluoro-L-phenylalanine (*21*) into melanomas was mediated by melanin synthesis as well as by increased amino acid transport associated with cell proliferation. The accumulation of phenylalanine analogs into various tumors was suggested to be mediated by increased amino acid transport.

L-[2-^{18}F]fluorophenylalanine (^{18}F-Phe) was developed and used to study the transport of brain amino acids (*22,23*), but has never been evaluated as a tumor imaging agent except in preliminary brain tumor imaging (*24*). To overcome the disadvantages of the short half-life of ^{11}C-Met, while preserving the characteristics of an amino acid tracer, we studied ^{18}F-Phe as a possible tumor imaging tracer and compared the results with ^{14}C-Met.

MATERIALS AND METHODS

The experimental protocol was approved by the Laboratory Animal Care and Use Committee of Tohoku University.

Radiopharmaceuticals

Fluorine-18-Phe was synthesized according to the method of Murakami et al. (*22*) with a specific activity of 23–38 GBq/mmole and radiochemical purity ≥99%. Briefly, L-phenylalanine was fluorinated by [^{18}F]acetylhypofluoride and ^{18}F-Phe was purified from the fluorinated mixture by high-performance liquid chromatography. L-[methyl-^{14}C]-methionine (^{14}C-Met, specific activity 2.15 GBq/mmole) as a substitute for ^{11}C-Met. [6-^{3}H]thymidine (^{3}H-Thd, specific activity: 962 GBq/mmole) and [2-^{14}C]thymidine (^{14}C-Thd, specific activity: 2.1 GBq/mmole) were obtained commercially.

Time-course of Tissue Distribution

Seven-week-old male Donryu rats were transplanted with 0.1 ml suspension of 10^7 AH109A hepatoma cells injected subcutaneously in the thigh region. Tracer experiments were performed 8 days after tumor transplantation following 8 hr of fasting. Twenty-one rats bearing AH109A tumor were injected intravenously into the lateral tail vein with a mixture of 1.11 MBq (30 μCi) ^{18}F-Phe and 178 kBq (4.8 μCi) each ^{14}C-Met and ^{3}H-Thd in 0.25 ml of saline and killed 5 (n = 4), 15 (n = 4), 30 (n = 4), 60 (n = 6), and 120 (n = 3) min later. Tissue samples were excised and weighed, and ^{18}F radioactivity was measured using an automated gamma-scintillation counter. One week later, tissue samples were processed and ^{3}H and ^{14}C radioactivity was measured using a liquid scintillation counter with a double-window technique, as previously described (*16*). Tissue radioactivity was expressed as the differential uptake ratio (DUR).

$$\text{DUR} = \frac{\text{Tissue radioactivity/Tissue weight}}{\text{Injected radioactivity/Animal weight}}. \qquad \text{Eq. 1}$$

Differences between two sets of data were tested for statistical significance using the Student's t-test.

Radiotherapy Monitoring Study

Animals were irradiated when tumors grew to 1.0–1.5 cm in diameter. Rats were anesthetized with intraperitoneal injection of sodium pentobarbital. Thigh tumors were exposed to a single dose of 20 Gy ^{60}Co irradiation, as described previously (*25*). Nonirradiated tumors in rats handled in the same manner, including anesthesia, were used as control. The tracer mixture of ^{18}F-Phe, ^{14}C-Met and ^{3}H-Thd was administered to three groups of 8 rats at 1, 3 and 6 days after irradiation and also to a control group of 6 rats. Rats were killed 60 min later and tissue radioactivity was measured as previously described.

Double-Tracer Macroautoradiography (ARG)

Four rats bearing AH109A tumors were injected with a mixture of either 111 MBq (3 mCi) ^{18}F-Phe and 1.11 MBq (30 μCi) ^{14}C-Met or ^{18}F-Phe and 1.11 MBq (30 μCi) ^{14}C-Thd and killed 1 hr later. The tumors were dissected and frozen for sectioning as previously reported (*26*). Several 5-μm thick sections were mounted on clean glass slides, air-dried and placed in direct contact with ARG films for 2 hr to produce ^{18}F-Phe images. One week later, following the decay of ^{18}F, the same sections were placed in contact with separate films for 14 days to produce ^{14}C-Met or ^{14}C-Thd images.

Whole-body ARG

Three rats bearing AH109A tumors in the back were injected with 185 MBq (5 mCi) ^{18}F-Phe, and two rats with 555 kBq (15 μCi) ^{14}C-Met, and killed 1 hr later by an overdose of chloroform anesthesia. The rats were embedded, frozen and sectioned as previously reported (*27*). Several 20-μm thick sections were placed on adhesive tape, mounted on cardboard, covered with thin polystyrene film, placed in contact with ARG films in cassettes and stored at −20°C. Fluorine-18-Phe images were obtained with 4.5-hr exposure. Carbon-14-Met images were obtained with 14-day exposure.

RESULTS

The time course of tissue distribution of ^{18}F-Phe is shown in Figure 1A. The highest uptake was in the pancreas, reaching a peak level 60 min postinjection, which then decreased at 120 min. Small intestine uptake showed a gradual increase for 120 min. Tumor uptake of ^{18}F-Phe was the second highest and peaked at 60 min. Tumor uptake was significantly higher than that of the liver at 30 and 60 min ($p < 0.02$), and the small intestine and kidney at 60 min ($p < 0.001$ each). The uptake of ^{18}F-Phe in the kidney, lung, brain, myocardium and muscle, and blood levels of ^{18}F-Phe were significantly lower than tumor uptake at all measured time intervals. The tumor-to-blood

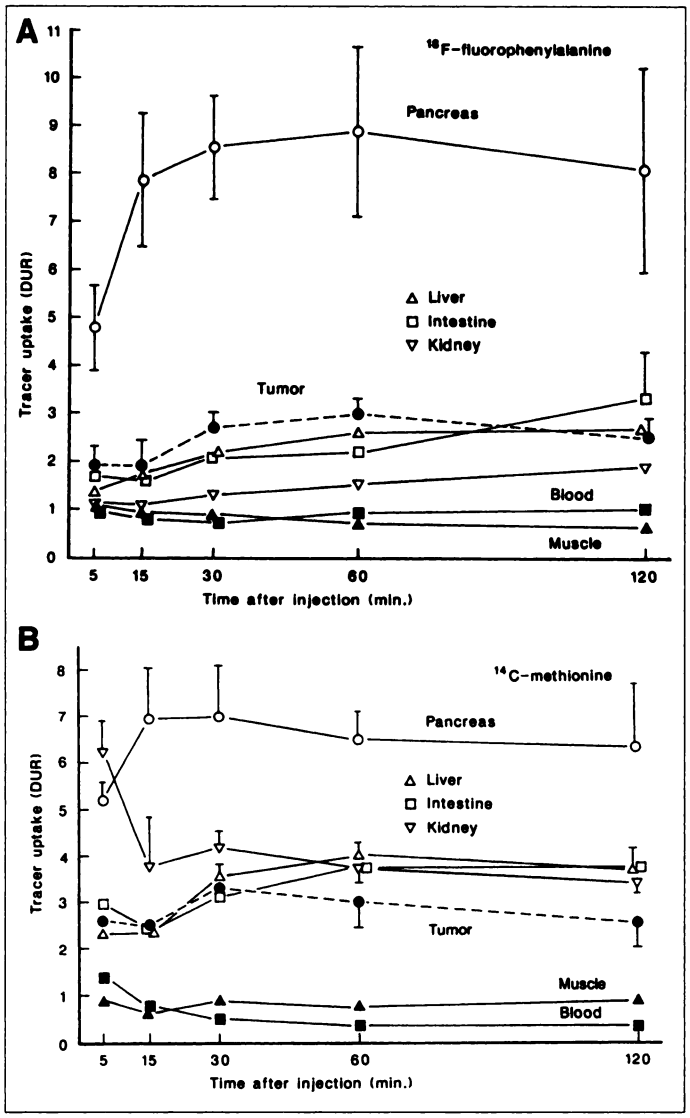

FIGURE 1. (A) Time course of tissue distribution of ^{18}F-Phe using the AH109A tumor in Donryu rats. Mean and s.d. of four to six rats. (B) Time course of tissue distribution of ^{14}C-Met using the AH109A tumor in Donryu rats performed as a multiple tracer study.

uptake ratio 60 min after injection of ^{18}F-Phe was 3.35, while the tumor-to-muscle ratio was 3.87 (Table 1).

Tissue distribution of ^{18}F-Phe was compared with that of ^{14}C-Met (Fig. 1B and Table 2). Tumor uptake of ^{14}C-Met peaked at 30 min and tended to decrease, although insignificantly, after that time. It was similar to the tumor uptake of ^{18}F-Phe at 60 min. Tumor uptake of ^{14}C-Met was lower than that of the intestines ($p < 0.05$) and pancreas ($p < 0.001$, $p < 0.02$) at 60 and 120 min, and lower than that of the liver ($p < 0.005$) and kidney ($p < 0.05$) at 60 min. The blood level of ^{14}C-Met decreased rapidly and became lower than that of ^{18}F-Phe at 30 ($p < 0.002$), 60 and 120 min ($p < 0.001$ each). This resulted in a higher tumor-to-blood ^{14}C-Met uptake ratio (8.47) and tumor-to-muscle ratio (4.07) at 60 min compared with that of ^{18}F-Phe at the same time interval. Brain uptake of ^{14}C-Met was lower than that of ^{18}F-Phe at 5 to 60 min ($p < 0.001$) and 120 min ($p < 0.002$), resulting in a higher tumor-to-brain ^{14}C-Met uptake ratio compared with that of ^{18}F-Phe (7.26 versus 3.97 at 60 min). On the other hand, ^{3}H-Thd uptake by the tumor was lower than ^{18}F-Phe and ^{14}C-Met ($p < 0.001$ at 60 min, Table 3).

The results of radiotherapy monitoring study are shown in Figure 2. Irradiation caused a rapid reduction in tumor uptake of all tracers. Tritium-Thd uptake by the tumor was lower than others but showed a similar rapid decrease following irradiation. Tumor uptake decreased significantly to 65.4% ± 7.4% ($p < 0.02$ compared with ^{14}C-Met), 66.5% ± 8.6% ($p < 0.05$ compared with ^{14}C-Met) and 77.1% ± 8.7% of control levels of ^{18}F-Phe, ^{3}H-Thd and ^{14}C-Met, respectively, 1 day after irradiation. It decreased further to 36.2% ± 6.4%, 36.5% ± 7.6% and 44.2% ± 5.6% ($n = 8$ for each) of control levels of ^{18}F-Phe, ^{3}H-Thd and ^{14}C-Met, respectively, 3 days after irradiation. No significant decline in the uptake was observed after the third day of irradiation. Reduction in tumor uptake of ^{18}F-Phe due to irradiation was significantly faster than that of ^{14}C-Met but was equivalent to that of ^{3}H-Thd. All these three tracers showed faster response after irradiation than FDG (1 day: 87.9% ± 18.2%, 3 days, 62.8% ± 13.7% of the control), as demonstrated in our previous study using the same tumor radiotherapy model (*16*). The muscle uptake and blood level of all three tracers were constant during this period (Fig. 2).

TABLE 1
Tissue Distribution of Fluorine-18-Fluorophenylalanine in Rats

	Time after injection (min)				
	5 (n = 4)	15 (n = 4)	30 (n = 4)	60 (n = 6)	120 (n = 3)
Lung	1.17 ± 0.05	0.98 ± 0.04	0.94 ± 0.03	1.01 ± 0.06	1.02 ± 0.08
Pancreas	4.79 ± 0.99	7.85 ± 1.44	8.54 ± 1.11	8.86 ± 1.89	8.06 ± 2.16
Intestine	1.69 ± 0.46	1.63 ± 0.43	2.10 ± 0.50	2.18 ± 0.18	3.29 ± 0.99
Liver	1.38 ± 0.06	1.72 ± 0.08	2.14 ± 0.12	2.60 ± 0.09	2.69 ± 0.32
Kidney	1.15 ± 0.06	1.11 ± 0.06	1.28 ± 0.05	1.52 ± 0.09	1.89 ± 0.07
Brain	1.12 ± 0.06*	0.91 ± 0.08*	0.94 ± 0.06*	0.75 ± 0.04*	0.62 ± 0.02†
Tumor	1.91 ± 0.40	1.86 ± 0.55	2.71 ± 0.29	2.98 ± 0.29	2.53 ± 0.37
Tumor-to-Blood	1.93	2.27	3.52	3.35	2.53
Tumor-to-Muscle	1.69	1.94	3.01	3.87	3.89

*$p < 0.001$ compared to ^{14}C-Met data in Table 2.
†$p < 0.002$ compared to ^{14}C-Met data in Table 2 (Student's t-test).
Data are mean ± s.d. of the differential uptake ratio. Number of animals are in parentheses. At 60 min, tumor-to-liver; $p < 0.02$, tumor-to-intestine and tumor-to-kidney, $p < 0.001$.

TABLE 2
Tissue Distribution of Carbon-14-L-Methionine in Rats

	Time after injection (min)				
	5 (n = 4)	15 (n = 4)	30 (n = 4)	60 (n = 6)	120 (n = 3)
Lung	2.09 ± 0.21	1.31 ± 0.16	1.08 ± 0.19	1.09 ± 0.10	1.01 ± 0.11
Pancreas	5.20 ± 0.38	6.95 ± 1.08	6.98 ± 1.11	6.49 ± 0.63	6.33 ± 1.41
Intestine	2.96 ± 0.36	2.39 ± 0.74	3.15 ± 0.48	3.75 ± 0.42	3.75 ± 0.44
Liver	2.33 ± 0.21	2.32 ± 0.74	3.55 ± 0.27	4.01 ± 0.28	3.70 ± 0.48
Kidney	6.26 ± 0.63	3.77 ± 1.10	4.18 ± 0.38	3.75 ± 0.36	3.41 ± 0.22
Brain	0.45 ± 0.02*	0.36 ± 0.05*	0.45 ± 0.01*	0.42 ± 0.02*	0.46 ± 0.03†
Tumor	2.65 ± 0.14	2.50 ± 0.64	3.33 ± 0.37	3.05 ± 0.54	2.55 ± 0.55
Tumor-to-Blood	1.73	3.38	6.40	8.47	6.89
Tumor-to-Muscle	2.91	3.42	3.70	4.07	2.93

*$p < 0.001$ compared to ^{18}F-Phe data in Table 1.
†$p < 0.002$ compared to ^{18}F-Phe data in Table 1 (Student's t-test).
Data are mean ± s.d. of the differential uptake ratio. Number of animals are in parentheses. At 60 min, tumor-to-liver was $p < 0.005$, tumor-to-intestine and tumor-to-kidney, $p < 0.05$; tumor to pancreas, $p < 0.001$. At 120 min, tumor to pancreas; $p < 0.02$, tumor to intestine; $p < 0.05$, tumor to liver and to kidney; NS.

Figure 3 shows two sets of typical double-tracer macroautoradiograms of a section of AH109A tumor obtained 1 hr after injection of ^{18}F-Phe and ^{14}C-Met or ^{18}F-Phe and ^{14}C-Thd. High grain density was observed in high cell density areas both in the ^{18}F-Phe and ^{14}C-Met images. Lower density was usually observed in the central necrotic region and in the granulation tissue of the tumor rim. Although the spatial resolution of the images was different in ^{18}F compared with that in ^{14}C due to the different physical characteristics, ^{18}F-Phe and ^{14}C-Met showed almost identical distribution in the tumor. The tumor uptake density of ^{14}C-Thd was lower than ^{18}F-Phe and ^{14}C-Met, but the distribution of ^{18}F-Phe and ^{14}C-Thd was similar and the dense area was identical in both images as well as the combination of ^{18}F-Phe and ^{14}C-Met.

Figure 4A shows a whole-body ARG of ^{18}F-Phe and Figure 4B a whole-body ARG of ^{14}C-Met 1 hr postinjection. Whole-body ARG of ^{18}F-Phe revealed high uptake in the AH109A tumor transplanted on the back. The pancreas showed the highest radioactivity followed by ureter, nasal and pharyngeal mucous membranes, thyroid and skin, which were similar to the levels observed in the tumor. The submandibular gland and bone marrow showed lower radioactivity than the tumor. The liver and intestine had lower radioactivity than the tumor, while the muscle, brain, myocardium and lung showed the lowest uptake. Whole-body ARG of ^{14}C-Met (Fig. 4B) also showed high uptake in the tumor. The pancreas and intestinal wall showed higher uptake of ^{14}C-Met than the tumor. The liver and kidney showed similar high uptake to the tumor. The brain and lung showed the lowest uptake and were lower than the muscle.

DISCUSSION

Increased utilization of amino acids in tumors has been investigated for more than 40 yr. For example, increased protein synthesis by proliferating tumor cells in vivo (*28,29*) and amino acid transport by cancer cells in vitro (*30,31*), have been reported. Based on these facts, various positron-labeled amino acids have been used for tumor imaging. Carbon-11-Met is considered one of the best labeled amino acids for tumor imaging, as confirmed by comparative experimental and clinical studies (*11,32*). The accumulation of ^{11}C-Met into malignant tissue is thought to be due to amino acid metabolism of cancer cells, such as increased active transport and incorporation of amino acids into the protein fraction (*33*). Furthermore, increased transmethylation also occurs in cancer cells in vitro (*34*). Recent studies revealed that the uptake of Met by tissues reflected mainly that of amino acid active transport rather than the rate of protein synthesis (*35,36*). These studies also demonstrated that a rapid accumulation of free ^{14}C-Met in a large intracellular pool and time-related incorporation of pooled ^{14}C-Met into protein fractions. In fact, results of brain tumor PET studies suggest that the transport of amino acids is a factor more important than the protein synthesis rate in determining the distribution of the amino acid tracer of ^{11}C-Met into tumor tissue (*37*).

TABLE 3
Tissue Distribution of Tritiated Thymidine in Rats

	Time after injection (min)				
	5 (n = 4)	15 (n = 4)	30 (n = 4)	60 (n = 6)	120 (n = 3)
Lung	1.41 ± 0.14	0.89 ± 0.15	0.71 ± 0.05	0.63 ± 0.07	0.52 ± 0.04
Pancreas	2.96 ± 0.60	3.34 ± 0.40	3.13 ± 0.36	3.63 ± 0.87	2.69 ± 0.34
Intestine	2.22 ± 0.48	1.46 ± 0.21	1.54 ± 0.13	1.75 ± 0.23	1.59 ± 0.06
Liver	1.68 ± 0.17	1.90 ± 0.33	1.82 ± 0.07	1.93 ± 0.11	1.59 ± 0.20
Kidney	4.93 ± 0.44	3.14 ± 0.64	2.57 ± 0.38	2.28 ± 0.14	1.58 ± 0.10
Brain	0.32 ± 0.02	0.27 ± 0.06	0.29 ± 0.04	0.30 ± 0.01	0.30 ± 0.02
Tumor	1.54 ± 0.20	1.66 ± 0.38	1.60 ± 0.20	1.89 ± 0.24	1.13 ± 0.23
Tumor-to-Blood	1.54	2.91	3.56	6.52	4.91
Tumor-to-Muscle	2.33	3.02	2.96	3.94	2.40

Data are mean ± s.d. of the differential uptake ratio. Number of animals are in parentheses.

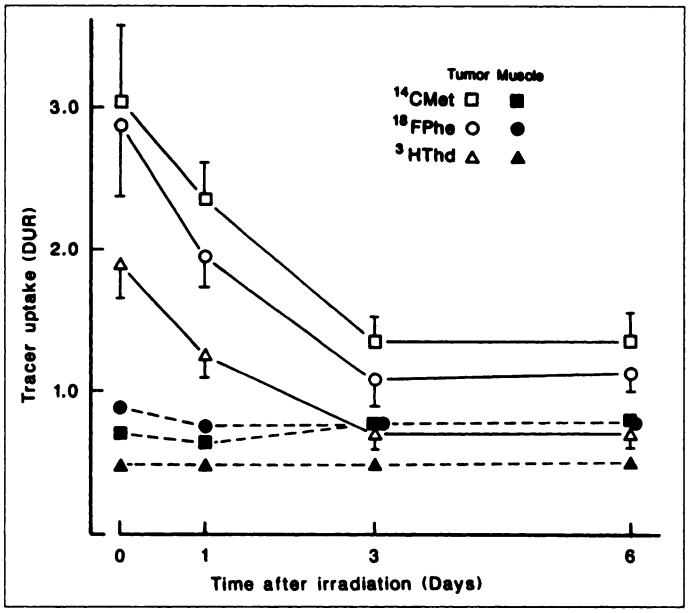

FIGURE 2. Results of radiotherapy monitoring study using ^{18}F-Phe, ^{14}C-Met and ^{3}H-Thd. Before (Day 0) and after 20 Gy of a single dose of ^{60}Co radiotherapy. AH109A tumor uptake of tracers was studied serially. Each point represents the mean and s.d. of eight rats. The tumor on the right thigh was irradiated while uptake by the muscle from the nonirradiated left thigh was used for comparison.

Fluorine-18-Phe was initially developed more than 20 yr ago as a possible pancreas imaging agent (*38*). Recently, Murakami et al. (*22*) developed an effective method for the synthesis of ^{18}F-Phe and studied its metabolism in the rat brain. The slow metabolism of ^{18}F-Phe, compared with natural Phe, suggests that ^{18}F-Phe is a suitable tracer for evaluation of amino acid transport to the brain (*23*). The transport of ^{18}F-Phe through the blood-brain barrier is mediated by the large neutral amino acid (NAA) transport system, used in transporting Met (*39*). Moreover, PET has been used to study the effect of aging on the transport of ^{18}F-Phe into the brain (*40*). Sharing the same membrane transport system with Met, ^{18}F-Phe is thus likely to

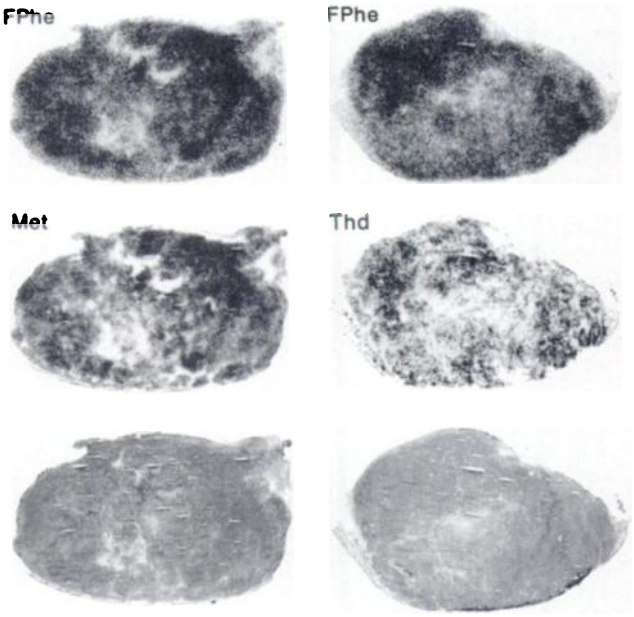

FIGURE 3. Two sets of double-tracer macroautoradiograms of AH109A tumor. Top and middle are double-tracer ARG, bottom is the histological section of the tumor stained with hematoxylin. Left column: a combination of ^{18}F-Phe and ^{14}C-Met. Right column: combination of ^{18}F-Phe and ^{14}C-Thd.

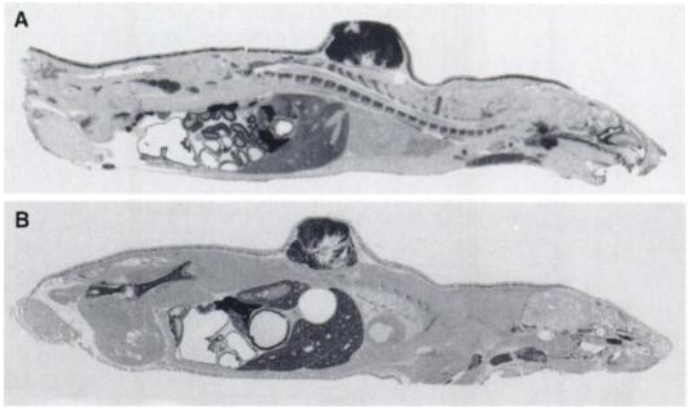

FIGURE 4. (A) Typical whole-body ARG of ^{18}F-Phe using a Donryu rat bearing an AH109A tumor on the back. Note the higher tracer concentration in the tumor compared with that in the liver. (B) Whole-body autoradiogram of ^{14}C-Met in a Donryu rat bearing a AH109A tumor on the back. Although these two whole-body ARGs are not the double-tracer study but rather from two different rats, lower tumor-to-liver contrast in ^{14}C-Met is evident compared with that of ^{18}F-Phe.

detect tumors and monitor treatment in a manner similar to that of Met. In this regard, preliminary PET studies of brain tumor using ^{18}F-Phe have demonstrated a high tumor-to-normal brain contrast, suggesting that ^{18}F-Phe may be useful for imaging brain tumors (*24,37*). Our present results demonstrated that the tumor-to-brain uptake ratio of ^{14}C-Met was higher than that of ^{18}F-Phe. This finding indicates that ^{11}C-Met may be superior to ^{18}F-Phe for brain tumor imaging. Our study also demonstrated a unique property for ^{18}F-Phe to detect the body tumors, including a rapid response of tumor ^{18}F-Phe uptake to radiotherapy as well as Met and Thd and identical intratumoral distribution of ^{18}F-Phe, Met and Thd.

In this study, we could not compare the distribution of ^{14}C-Met and ^{14}C-Thd directly in the same tumor section. A similar distribution of ^{14}C-Met and ^{14}C-Thd, however, in each tumor image was observed. These findings support our previous studies, in which both ^{3}H-Thd (*26*) and ^{14}C-Met (*17*) were detected in viable malignant cells.

The high false FDG uptake observed in several patients following radiotherapy suggests the accumulation of FDG in inflammatory tissue after radiotherapy. In support of this argument, autoradiography studies have demonstrated high accumulation of FDG in macrophages and young granulation tissue (*26*). A change in tumor uptake of ^{11}C-Met after radiotherapy, a tracer more sensitive and faster than FDG (*16*), is not affected by inflammatory reactions (*41*). The low concentration of Met in non-neoplastic tissue makes it a suitable tracer for treatment evaluation (*17*). Macroautoradiography in the present study clearly demonstrated an identical distribution of ^{18}F-Phe and ^{14}C-Met and a faster response of tumor uptake of ^{18}F-Phe after radiotherapy compared with that of ^{14}C-Met.

Our results demonstrated that AH109A tumor uptake of ^{18}F-Phe was higher than that of the liver, intestine and kidneys. The high tumor uptake of ^{18}F-Phe is probably due to increased transport of amino acids. A positive contrast of tumors in some abdominal organs was obtained with ^{18}F-Phe but not ^{14}C-Met. Liver uptake of ^{18}F-Phe was significantly less than that of Met at 30 and 60 min, causing higher pancreas-to-liver and tumor-to-liver ratios for ^{18}F-Phe. A similar low liver uptake has been reported in other tracers for amino acid transport, such as ^{11}C-aminocyclopentanecarboxylic acid and its derivatives (*11,42*). The dissociation of a high tumor and pancreas uptake and a low liver uptake was observed in common with these tracers. This observation may be due to differences in cell

membrane function. Although the mechanism is not clear, the low liver uptake gives ^{18}F-Phe an advantage over Met for imaging abdominal malignancies.

CONCLUSION

Fluorine-18-Phe seems to be a potentially useful amino acid tracer for tumor imaging, with a longer half-life compared to ^{11}C-Met. Its distribution is identical to ^{14}C-Met in tumor tissues and it has a similar sensitive response of tumor ^{18}F-Phe uptake to radiotherapy.

ACKNOWLEDGMENTS

The authors thank Mr. Y. Sugawara for photography, Mr. T. Sato, Dr. T. Akaizawa and Dr. R. Goto for assistance and the staff of the Cyclotron and Radioisotope Center, Tohoku University for their cooperation. We also thank Dr. F.G. Issa (Word-Medex) for his assistance in reading and editing the manuscript. This work was supported by grants-in-aid (04557047, 06454320, 06670899) from the Japanese Ministry of Education, Science and Culture.

REFERENCES

1. Bergström M, Collins VP, Ehrin E, et al. Discrepancies in brain tumor extent as shown by computed tomography and positron emission tomography using [^{68}Ga]EDTA, [^{11}C]glucose and [^{11}C]methionine. *J Comput Assist Tomogr* 1983;7:1062–1066.
2. Leskinen-Kallio S, Någren K, Lehikoinen P, Ruotsalainen U, Teräs M, Joensuu H. Carbon-11-methionine and PET is an effective methods to image head and neck cancer. *J Nucl Med* 1992;33:691–695.
3. Kubota K, Matsuzawa T, Ito M, et al. Lung tumor imaging by positron emission tomography using ^{11}C-L-methionine. *J Nucl Med* 1985;26:37–42.
4. Leskinen-Kallio S, Någren K, Lehikoinen P, Ruotsalainen U, Joensuu H. Uptake of ^{11}C-methionine in breast cancer studied by PET. An association with the size of S-phase fraction. *Br J Cancer* 1991;64:1121–1124.
5. Leskinnen-Kallio S, Ruotsalainen U, Någren K, Teräs M, Joensuu H. Uptake of carbon-11-methionine and fluorodeoxyglucose in non-Hodgkin's lymphoma: a PET study. *J Nucl Med* 1991;32:1211–1218.
6. Ogawa T, Shishido F, Kanno I, et al. Cerebral glioma: evaluation with methionine PET. *Radiology* 1993;186:45–53.
7. Di Chiro G, DeLaPaz RL, Brooks RA, et al. Glucose utilization of cerebral gliomas measured by [^{18}F]fluorodeoxyglucose and positron emission tomography. *Neurology* 1982;32:1323–1329.
8. Yonekura Y, Benua RS, Brill AB, et al. Increased accumulation of 2-deoxy-[2-^{18}F]fluoro-D-glucose in liver metastasis from colon cancer. *J Nucl Med* 1982;23:1133–1137.
9. Bares R, Klever P, Hauptmann S, et al. Fluorine-18-fluorodeoxyglucose PET in vivo evaluation of pancreatic glucose metabolism for detection of pancreatic cancer. *Radiology* 1994;192:79–86.
10. Syrota A, Duquesnoy N, Paraf A, Kellershohn C. The role of positron emission tomography in the detection of pancreatic disease. *Radiology* 1982;143:249–253.
11. Kubota K, Yamada K, Fukuda H, et al. Tumor detection with carbon-11-labeled amino acids. *Eur J Nucl Med* 1984;9:136–140.
12. Bergström M, Muhr C, Lundberg PO, et al. Rapid decrease in amino acid metabolism in prolactin-secreting pituitary adenomas after bromocriptine treatment: a PET study. *J Comput Assist Tomogr* 1987;11:815–819.
13. Derlon JM, Bourdet C, Bustany P, et al. Carbon-11-L-methionine uptake in gliomas. *Neurosurgery* 1989;25:720–728.
14. Kubota K, Yamada S, Ishiwata K, et al. Evaluation of the treatment response of lung cancer with positron emission tomography and L-[methyl-^{11}C]methionine: a preliminary study. *Eur J Nucl Med* 1993;20:495–501.
15. Huovinen R, Leskinen-Kallio S, Någren K, Lehikoinen P, Ruotsalainen U, Teräs M. Carbon-11-methionine and PET in evaluation of treatment response of breast cancer. *Br J Cancer* 1993;67:787–791.
16. Kubota K, Ishiwata K, Kubota R, et al. Tracer feasibility for monitoring tumor radiotherapy: A quadruple tracer study with fluorine-18-fluorodeoxyglucose or fluorine-18-fluorodeoxyuridine, L-[methyl-^{14}C]methionine, [6-^{3}H]thymidine, and gallium-67. *J Nucl Med* 1991;32:2118–2123.
17. Kubota R, Kubota K, Yamada S, et al. Methionine uptake by tumor tissue: a microautoradiographic comparison with FDG. *J Nucl Med* 1995;36:484–492.
18. Coenen HH, Kling P, Stocklin G. Cerebral metabolism of L-[2-^{18}F]fluorotyrosine: a new PET tracer of protein synthesis. *J Nucl Med* 1989;30:1367–1372.
19. Wienhard K, Herholz K, Coenen HH, et al. Increased amino acid transport into brain tumors measured by PET of L-[2-^{18}F]fluorotyrosine. *J Nucl Med* 1994;32:1338–1346.
20. Kubota R, Yamada S, Ishiwata K, Kubota K, Ido T. Active melanogenesis in non-S-phase melanocytes in B16 melanomas in vivo investigated by double-tracer microautoradiography with ^{18}F-fluorodopa and ^{3}H-thymidine. *Br J Cancer* 1992;66:614–618.
21. Kubota R, Yamada S, Ishiwata K, Tada M, Ido T, Kubota K. Cellular accumulation of ^{18}F-labeled boronophenylalanine depending on DNA synthesis and melanin incorporation: a double-tracer microautoradiographic study of B16 melanomas in vivo. *Br J Cancer* 1993;67:701–705.
22. Murakami M, Takahashi K, Kondo Y, et al. The comparative synthesis of ^{18}F-fluorophenylalanines by electrophilic substitution with ^{18}F-F_2 and ^{18}F-AcOF. *J Lab Compd Radiopharm* 1988;25:573–578.
23. Murakami M, Takahashi K, Kondo Y, et al. The slow metabolism of L-[2-^{18}F]-fluorophenylalanine in rat. *J Lab Compd Radiopharm* 1989;27:245–255.
24. Shishido F, Murakami M, Miura S, et al. Clinical investigation of ^{18}F-fluorophenylalanine for brain tumor imaging. Comparison with ^{11}C-methionine (in Japanese). *Jpn J Nucl Med* 1988;25:1431–1435.
25. Kubota K, Matsuzawa T, Takahashi T, et al. Rapid and sensitive response of carbon-11-L-methionine tumor uptake to irradiation. *J Nucl Med* 1989;30:2012–2016.
26. Kubota R, Yamada S, Kubota K, Ishiwata K, Tamahashi N, Ido T. Intratumoral distribution of fluorine-18-fluorodeoxyglucose in vivo: high accumulation in macrophages and granulation tissue studied by microautoradiography. *J Nucl Med* 1992;33:1972–1980.
27. Kubota K, Matsuzawa T, Fujiwara T, et al. Differential diagnosis of AH109A tumor and inflammation by radioscintigraphy with L-[methyl-^{11}C]methionine. *Jpn J Cancer Res* 1989;80:778–782.
28. Busch H, Davis JR, Honig GR, Anderson DC, Nair PV, Nyhan WL. The uptake of a variety of amino acids into nuclear proteins of tumors and other tissues. *Cancer Res* 1959;19:1030–1039.
29. Wagle SR, Morris HP, Weber G. Comparative biochemistry of hepatomas V. Studies on amino acid incorporation in liver tumors of different growth rates. *Cancer Res* 1963;23:1003–1007.
30. Foster DO, Pardee AB. Transport of amino acid by confluent and nonconfluent 3T3 and polyoma virus-transformed 3T3 cells growing on glass cover slips. *J Biol Chem* 1969;244:2675–2681.
31. Isselbacher KJ. Increased uptake of amino acids and 2-deoxy-D-glucose by virus-transformed cells in culture. *Proc Nat Acad Sci USA* 1972;69:585–589.
32. Kubota K, Matsuzawa T, Fujiwara T, et al. Differential diagnosis of lung tumor with positron emission tomography: a prospective study. *J Nucl Med* 1990;31:1927–1933.
33. Ishiwata K, Vaalburg W, Elsinga PH, Paans AMJ, Woldring MG. Comparison of L-[1-^{11}C]methionine and L-methyl-[^{11}C]methionine for measuring in vivo protein synthesis rates with PET. *J Nucl Med* 1988;29:1419–1427.
34. Stern PH, Wallace CD, Hoffman RM. Altered methionine metabolism occurs in all members of a set of diverse human tumor cell lines. *J Cell Physiol* 1984;119:29–34.
35. Ishiwata K, Kubota K, Murakami M, et al. Re-evaluation of amino acid PET studies: can the protein synthesis rates in brain and tumor tissues be measured in vivo? *J Nucl Med* 1993;34:1936–1943.
36. Ishiwata K, Kubota K, Murakami M, Kubota R, Senda M. A comparative study on protein incorporation of L-[methyl-^{3}H]methionine, L-[1-^{14}C]leucine and L-[2-^{18}F]fluorotyrosine in tumor bearing mice. *Nucl Med Biol* 1993;20:895–899.
37. Miura S, Murakami M, Kanno I, et al. Kinetic analysis of L-2-[^{18}F]-fluorophenylalanine in human brain using quantitative dynamic PET. *J Cereb Blood Flow Metab* 1989;9:S47.
38. Hoyte RM, Lin SS, Christman DR, Atkins HL, Hause W, Wolf AP. Organic radiopharmaceuticals labeled with short lived nuclides 3. Fluorine-18-labeled phenylalanines. *J Nucl Med* 1971;12:280–286.
39. Nakamichi H, Murakami M, Miura S, Kondoh Y, Mizusawa S, Ono Y. L-[2-^{18}F]fluorophenylalanine and L-[U-^{14}C]phenylalanine: a comparative study of their transport to rat brain. *Nucl Med Biol* 1993;20:95–99.
40. Ito H, Hatazawa J, Murakami M, et al. Aging effect of amino acid transport from blood to brain in humans—a PET study. *J Cereb Blood Flow Metab* 1993;13:S399.
41. Kubota K, Kubota R, Yamada S, Tada M. Effects of radiotherapy on the cellular distribution of L-methionine in tumor tissue. *Nucl Med Biol* 1995;22:193–198.
42. Washborn LC, Sun TT, Anon JB, Hayes RL. Effect of structure on tumor specificity of alicyclic-amino acids. *Cancer Res* 1978;38:2271–2273.